Developmental loss of oligodendrocytes exacerbates adult CNS demyelination

Ahdeah Pajoohesh-Ganji (ahdeah@gwu.edu)
George Washington University https://orcid.org/0000-0002-1542-029X
Molly Karl
George Washington University
Eric Garrison
George Washington University
Cheryl Clarkson-Paredes
George Washington University
Julie Ahn
George Washington University
Robert H. Miller
George Washington University

Research

Keywords: multiple sclerosis, oligodendrocytes, demyelination, priming, glial activation, EAE, LPC

Posted Date: November 22nd, 2019

DOI: https://doi.org/10.21203/rs.2.17630/v1

Abstract

Background Multiple sclerosis (MS), a neurodegenerative autoimmune disease characterized by loss of oligodendrocytes and myelin in the brain and spinal cord, results in localized functional deficits. Several risk factors have been associated with MS, however none can fully explain an enhanced susceptibility. Epidemiological data, based on geographical prevalence studies suggest susceptibility is established early in life and frequently long before disease diagnosis implicating developmental events influence adult disease progression. Here we test the hypothesis that loss of mature oligodendrocytes during postnatal development results in enhanced susceptibility to an adult demyelinating insult. Methods A transgenic mouse model was utilized to specifically induce apoptosis in a subset of mature oligodendrocytes (MBP-iCP9) during the first 2 postnatal weeks followed by either a local LPC spinal cord injection or the induction of EAE in the adult. Immunostaining, immunoblotting, behavioral testing, and electron microscopy were utilized to examine the differences between groups. Results We show that during development, oligodendrocyte apoptosis results in transient reductions in myelination and functional deficits that recover after 10-14 days. Compared to animals in which oligodendrocyte development was unperturbed, animals subjected to postnatal oligodendrocyte ablation showed delayed recovery from an LPC lesion. Unexpectedly, the induction and severity of EAE was not significantly altered in animals following oligodendrocyte ablation even though there was a substantial increase in spinal cord tissue damage and CNS inflammation. It is currently unclear why these changes are not reflected in enhanced functional deficits. Conclusions These observations suggest that developmental loss of oligodendrocytes results in long lasting tissue changes that alter its capacity for repair in the adult.

Introduction

Multiple sclerosis (MS) is characterized by oligodendrocyte loss, demyelination, microglial activation, immune cell infiltration, and inflammation that are correlated with functional deficits. A variety of risk factors including gender, genetics, vitamin D deficiency, race and certain viral infections have been associated with MS [1] while epidemiological studies indicate that environmental factors early in life influences the development of the adult disease [2]. The concept that early insults influence the progression of adult disease is not restricted to MS and has been proposed for a number of diseases including Crohn's disease [3], asthma [4], and autism [5], where exposure to an insult such as infectious agents early in development has a lasting influence on the neuroimmune responses [6] and cognitive functions that become apparent following a second adult challenge or insult [7, 8]. Mechanistically, this has been proposed to present a priming phenomenon reflecting a phenotypic alteration in the microglial population characterized by increases in interleukin-1 beta (IL-1β) production [9]. It is likely however, that priming also involves other cell types and occurs in response to a broad range of other developmental perturbations.

In the current study, we utilized a transgenic mouse model (MBP-iCP9) which expresses an inducible form of caspase 9 (iCP9) driven by a fragment of the MBP promoter to specifically target apoptosis in a

subpopulation of mature oligodendrocytes [10, 11] during development. Crosslinking iCP9, through local delivery of a chemical inducer of dimerization (CID), results in activation of the caspase pathway and the apoptosis of mature oligodendrocytes without directly affecting other central nervous system (CNS) cell types [12, 13]. Combining early oligodendrocyte ablation with either spinal cord lysophosphatidylcholine (LPC, lysolecithin) lesion or the induction of experimental autoimmune encephalomyelitis (EAE) in adults, we show that while early ablation of oligodendrocytes results in a reduction in myelin and functional deficits, these recover relatively rapidly. Developmental loss of oligodendrocytes does however significantly impair recovery and increases CNS immunoreactivity in mature animals following either LPC or EAE induced damage. Together these studies support the notion that damage to the oligodendrocyte lineages early in development enhances the susceptibility to demyelinating insults in the adult CNS.

Materials And Methods

Animals and *in vivo* injections. All the studies comply with the George Washington University Medical Center Institutional Animal Care and Use Committee guidelines. Both male and female MBP-iCP9 transgenic mice [10] on a C57Black6 background were used throughout this study. Due to the limited number of transgenic pups, we were unable to perform gender specific studies although no obvious differences were detected. For the EAE induction studies, only female mice were used per manufacturer's instruction (Hook Laboratories; # EK-2110).

Pups were injected subcutaneously with 100 mg/Kg body weight of CID (clontech laboratories; #635069) daily for 7 days starting on postnatal day 4 or every other day for a total of 7 injections. CID stock solution was made in 100% ethanol and diluted in equal volume of Polyethylene Glycol (PEG400, Fisher Scientific; #P167) and 1% Tween-20 in PBS. Controls were injected with vehicle lacking CID, where 100% ethanol was added to PEG400 and 1% Tween-20 in PBS. Under terminal sedation, mice were sacrificed 2 weeks after the LPC and 4 weeks after the EAE studies and transcardially perfused with 1xPBS followed by fixative. Animals were fixed with either 4% paraformaldehyde (PFA) for immunefluorescence staining or 4% paraformaldehyde-2% glutaraldehyde-0.1 M sodium Cacodylate (PFA/GA) for Scanning Electron Microscopy (SEM). A minimum of 3 animals were used for each study.

LPC surgeries. Male and female pups were injected with vehicle or CID, allowed to mature to 6-7 weeks of age, and a spinal cord LPC lesion performed at T10 and T11 as previously described [11]. Animals were allowed to recover for 14 days before analysis.

EAE induction. Female vehicle or CID injected pups were allowed to mature to 10-11 weeks at which point EAE was induced accordingly to the manufacturer's guidelines (Hooke Laboratories #EK-2110). Animals showed symptoms of EAE approximately 8 days after induction and were scored on daily basis according to the following criteria: 1 loss of tail tonicity or hind limb weakness to 5 severe paralysis or death (Table 1). Animals scored 3 or higher were given 0.2 ml saline to prevent dehydration.

Open field testing. For functional testing, mice were placed in a Plexiglas open field (Med Associates, St Albans, VT, USA) outfitted with photobeam detectors, and their activity was monitored using the activity

monitoring software (Med Associates). Mice were allowed to habituate in the open field for 10 min and total distance traveled and speed were recorded [14].

Tissue processing. Tissues were processed for 3 different procedures. 1) *Immunofluorescence staining*: animals were fixed with PFA and spinal cords were cryoprotected using 10, 20, and 30% sucrose gradient in 1xPBS solutions; sections were cut at 20 μm. 2) *Electron Microscopy*: animals were fixed with PFA/GA and spinal cords were cut to 400 μm sections before processing. Sections were then osmicated (1% OsO_4) for at least 4 hours followed by 1% uranyl acetate overnight. After gradated dehydration with ethanol and propylene oxide, sections were placed in Epon812 and cut at 1 μm or 120 nm using an ultramicrotome (Leica UC6). Some sections were stained with Solochrome or Toluidine Blue staining to visualize myelin and some were placed on semiconductor grade Si-wafer microtome. 3) *Immunoblotting*: animals were perfused with cold 1xPBS and spinal cords were flash-frozen in liquid nitrogen and stored at -80 °C.

Immunostaining. Cross sections were rehydrated, blocked, and incubated with primary antibodies overnight followed by appropriate secondary antibodies for an hour prior to mounting. The following primary antibodies were used: MBP (1:300- Abcam; #7349), DsRed (1:400- Takara; #632496), Iba1 (1:500- WACO; #019-19741), and GFAP (1:500- Biolegend; #PRB-571C), PDGFαR (1:100- BD Biosciences; #558774), and CC1 (1:200- Millipore; #OP80). Appropriate secondary Alexa 488 or 594 (1:500) antibodies were used. Sections were counter-stained with Dapi (1:1000- Thermofisher; #46190) before mounting (Fluoromount G: Electron Microscopy Sciences; #17984-25).

Immunoblotting. Frozen tissues were processed and lysates were run on 4-20% gels (BioRad; #456-1094). The following primary antibodies were used: MAG (1:5000, Generous gift from Dr. Richard H. Quarles [15]), MBP (1:1000 for WB; Abcam; #7349), and Actin (1:2000; Santa Cruz; #SC47778) antibodies. Appropriate secondary antibodies were used at 1:5000.

Microscopy. Microscopy was performed at the Center for Microscopy and Image Analysis (CMIA) at the George Washington University Medical Center. Confocal microscopy images were captured using the Zeiss Cell Observer Z1 spinning disk confocal microscope (Carl Zeiss, Inc.) equipped with ASIMS-2000 (applied scientific Instrumentation) scanning stage with z-galvo motor, and Yokogawa CSU-X1 spinning disk. Zen Blue software (Carl Zeiss, Inc.) was used with 25x and 63x objectives to acquire tile images and produce maximum intensity projections. SEM was performed using a Helios NanoLab 660 SEM (Thermo Fisher, FEI) equipped with a concentric backscattering detector (CBS) using immersion mode for SEM high-resolution imaging. For the acquisition conditions, we used 2 kV with a landing current ranging from 0.2-0.4 nA with a working distance of 4 mm. For imaging, the entire spinal cord was tile-imaged at low magnification (600x) and fused into a single tiling map per sample and was used as a navigation map to identify lesioned areas (MAPS software). Then, high-resolution (3,500x or 15,000x) imaging was performed in the focus area at 10 ms dwell time and 20 mm horizontal field of view.

Statistical Analyses. All statistical tests were performed using the GraphPad Prism Program, Version 6 (GraphPad Software, Inc. San Diego, CA). A p value<0.05 was considered statistically significant and is demarked with an asterisk. NIH Image J was used to analyze pixel intensity for Western blot analysis. Photoshop was used to calculate the percent lesion and to count cells and the number of remyelinated axons in 3 random sites of the spinal cord under 63x magnification.

Results

Systemic injection of CID ablates oligodendrocytes throughout the CNS

In previous studies local injections of CID into MBP-iCP9 transgenic (TG) mice have been used to specifically ablate a proportion of oligodendrocytes locally in regions of the spinal cord [11], which ultimately recovers, and in the optic nerve [12, 13], where recovery is delayed. In the current study we assessed the effects of systemic loss of oligodendrocytes during development on myelination and on recovery in response to adult demyelinating insults. Systemic, subcutaneous-injection of CID into MBP-iCP9 animals for 7 consecutive days, starting 4 days after birth, results in significant decrease in the density of mature oligodendrocytes as detected by DsRed labeling in different areas of the brain including the corpus callosum and cerebellum (Figures 1A and B), the optic nerve (Figure 1C), and the spinal cord (Figure 1D) while TG controls were unaffected by vehicle injections. Similar levels of oligodendrocyte loss were seen in MBP-iCP9 animals that received daily or every other day (EOD) CID injections and all subsequent studies were performed on animals receiving alternate daily injections (Figures 2A, B). Myelin perturbation in oligodendrocyte ablated mice resulted in reduced MBP staining throughout the CNS (Figure 1) and a significant decrease in the level of the myelin proteins MAG and MBP in spinal cord tissues (Figure 2D). No significant regional differences were seen in the response to systemic CID delivery. All regions of the CNS showed reductions in myelin intensity (Figure 1) and an approximately 50% reduction in the number of CC1+ oligodendrocytes after CID injections (Figures 2A and C).

Systemic oligodendrocytes ablation leads to myelin loss, glial activation and transient functional deficits

To further assess the effect of oligodendrocyte ablation on myelin formation, spinal cord sections from experimental and control animals were stained with Solochrome 3 days after the final injection and the relative intensity assayed. Following CID injections, a reduction of approximately 50% in the level of Solochrome staining was apparent, particularly in the ventral spinal cord (Figure 3A), suggesting a reduction in myelin formation. Consistent with these observations, ultrastructural analysis showed a 50% reduction in the number of myelinated axons (Figure 3B) at P21. While vehicle treated animals had on average density of 48/100 μm^2 myelinated axons, in CID treated animals this was reduced to 26/100 μm^2 (p-value 0.0001). In general, the myelin that was present in CID treated animals appeared relatively normal and there were no significant differences in the G ratios. The loss of mature oligodendrocyte affected other glial populations. Three days after CID delivery, astrocytes were activated as indicated by an increase in the GFAP+ processes (Figure 3C), while microglial morphology changed from ramified to

amoeboid and an increase in Iba1 was observed suggesting their activation (Figure 3D). In addition, the number of PDGFRα+ oligodendrocyte progenitor cells (OPCs) was also increased following ablation of oligodendrocytes (Figure 3C).

The reduction in oligodendrocytes results in transient functional deficits. Following developmental ablation of mature oligodendrocytes between P4-P18, animals showed reduced mobility at P21 that had largely recovered one week later at P28 (Figure 4). For example, in open field studies, animals subjected to oligodendrocyte ablation showed a significant reduction in the total distance traveled compared to vehicle injected controls at P21 (Figures 4B and C). Similarly, the average speed of movement was significantly reduced in animals following oligodendrocyte ablation compared to vehicle-treated controls (Figure 4C). The changes in motility were transient and no significant differences between experimental and control animals were detected at P28. These data suggest oligodendrocyte ablation and reduction in CNS myelin impairs motor activity and that the functional recovery is consistent with a normalization of CNS myelin.

Early oligodendrocyte ablation delays adult remyelination.

Previous studies suggested that local ablation of oligodendrocytes resulted in impaired repair following an adult demyelinating lesion [11]. Interpretation of that data was, however complicated due to potential responses to the local CID injections. In the current study, subcutaneous systemic delivery of CID eliminates this complication. The rate of remyelination following a spinal cord LPC lesion was compared in CID and control animals (wild type mice injected with CID and TG mice injected with vehicle) at 6 weeks of age (Figure 5A). Injection of saline into wild type (WT/-/Saline) or MBP-iCP9 animals showed no significant demyelination (Figure 5B) as previously reported [11]. Comparison of the lesion area by Solochrome labeling 2 weeks after an LPC lesion demonstrated smaller residual lesions in control MBP-iCP9 animals that were developmentally treated with vehicle compare to those treated with CID (Figure 5B). To quantify differences in lesion size, the relative proportion of affected dorsal spinal cord white matter was assayed. No differences in total dorsal white matter area were seen between vehicle and CID injected animals (Figure 5C) and initial lesion formation was similar. By contrast, at 2 weeks post-lesion (pl) the proportion of lesion affected area was significantly different between vehicle and CID treated animals. The average lesion area constituted approximately 20% of dorsal white matter area in vehicle and approximately 40% in CID treated animals suggesting that systemic developmental depletion of oligodendrocytes inhibits adult myelin repair.

To directly assess remyelination, the morphology of lesions in vehicle and CID treated animals were assessed by Toluidine blue staining and ultrastructural analyses at 14dpl. Extensive remyelination was evident in vehicle treated animals. Profiles of thinly myelinated axons were distributed throughout the lesion particularly associated with blood vessels and the number of macrophage-like cells was relatively low. Ultrastructural analysis confirmed the presence of a significantly higher number of thinly remyelinated axons as compared to lesions from CID treated animals (p-value 0.02) (Figure 6). Lesions from CID treated animals also contained a greater density of phagocytic cells consistent with the

proposal that remyelination in the LPC model is impaired by developmental loss of mature oligodendrocytes.

Developmental oligodendrocyte ablation increases immune cell activation in EAE

Since developmental ablation of oligodendrocytes impaired remyelination in the LPC model, we examined its effects in the MOG_{35-55}-EAE animal model that is both more chronic and more immunologically based. Female MBP-iCP9 animals that had received either vehicle or CID injections during the P4-P18 developmental period were induced with EAE at 11 weeks of age and the development of the disease assayed for 28 days (Figure 7A). Comparison of the clinical scores showed no significant differences in the timing of onset of disease, the rate of increase in disease severity, or the final level of functional deficits between vehicle and CID treated animals (Figures 7B and C) suggesting that impairment of remyelination did not exacerbate disease progression. However, histological and immunological analysis of the spinal cord showed significant differences in vehicle and CID treated animals. The lesions in CID treated animals contained more degenerating axons with the residual myelin sheaths that were less well compacted compared to controls (Figure 7D). The level of inflammation in tissue from CID treated animals was higher than in controls. Elevated levels of astrocyte reactivity were evident through dramatic increases in expression of GFAP throughout the spinal cord (Figure 8). Similarly, elevated levels of microglial activation were evident by their increased number and the development of ameboid morphology (Figure 9). Together these data suggest that oligodendrocyte loss during development results in an elevated immune response in the EAE setting. Why such an increase in inflammation does not result in a worsening of the clinical score is currently unclear.

Discussion

Previous studies have utilized the MBP-iCP9 model to examine the mechanisms of cell death and the consequences of oligodendrocyte loss in the spinal cord and optic nerve [11-13]. These studies have largely relied on the local injection of CID that results in a local area of demyelination. In the current study we expand these observations in 3 ways. First, we show that systemic delivery of CID through a subcutaneous injection results in widespread reduction of myelin and loss of oligodendrocytes. Second, the loss of approximately 50% of oligodendrocytes and myelin during postnatal development compromises animal mobility. Third, while adult remyelination is negatively affected by early oligodendrocyte loss as seen in the LPC model, the functional outcome in EAE appears unaffected.

Apoptosis of oligodendrocytes during postnatal development has short-term and long-term impacts on CNS tissue. Exposure to CID in MBP-iCP9 animals results in the specific loss of mature oligodendrocytes through apoptosis [10], however the induction of cell death in oligodendrocytes has indirect effects on other neural cell populations. For example, CID induced-oligodendrocyte ablation results in an increase in PDGFRα+ OPCs in the spinal cord as well as activation of astrocytes reflected by an increased expression of GFAP immunoreactivity in their processes. The molecular basis of these changes is unclear. The increase in OPCs may reflect a negative feedback loop in which the loss of oligodendrocytes stimulates

the production of OPCs. Such a regulatory system has been proposed for OPCs [16, 17] and myelin is known to regulate OPC differentiation [18, 19]. Cells undergoing apoptosis have been shown to express signals (eat me) including phosphatidylserine (PS) and lysophospatidylcholine (LPC) that stimulate the phagocytic activity of nearby macrophages and microglia [20-22] and it seems likely that such signals may be responsible for astrocyte activation. Consistent with this hypothesis, 3 days after the last CID treatment, Iba1+ microglia in the spinal cord developed an amoeboid morphology suggesting their activation. Whether the loss of oligodendrocytes/myelin or activation of the innate immune system is responsible for the changes in animal motility is currently unclear although patients with minimal symptoms of MS also show a decrease in gait velocity, due to poor stability and this increases with disease progression [23]. Although the most obvious effects of oligodendrocyte loss on CNS tissue are transient, there are more subtle long-lasting effects. These are evident in the changes in myelin repair seen with LPC lesions and the enhanced inflammatory responses seen in EAE. Which cell population retains the memory of the first insult is unknown, but it is likely to be either astrocytes or microglia given their subsequent response to adult injury.

The concept that injuries, infection or other perturbations during postnatal development result in long-lasting changes in CNS immune cells has been proposed in other conditions. For instance, studies have shown that exposure to an insult such as an infectious agent early in development may influence neuroimmune responses [6] and cognitive functions in adulthood upon a second challenge or insult [7, 8]. This appears to reflect a priming phenomenon in microglia that results in morphological changes and increased microglial interleukin-1 beta (IL-1β) production [9]. Priming may occur as a result of changes in the microenvironment, which may involve other cell types in the CNS and not all the effects of priming require a second insult. Patients that suffer from traumatic brain injury may have long lasting changes in microglial cell functions [24]. Likewise, individuals subjected to concussion have an elevated level of microglial activation that leaves them susceptible to depression [24-26]. Several factors associated with the early loss of oligodendrocytes might impair remyelination and the functions of microglia in the adult. Exposure to dying oligodendrocytes may prime local microglia to retain an activated state and in response to a second stimulus, they elevate the production of proinflammatory cytokines [9] that impair recovery. Alternatively, exposure of microglia to oligodendrocyte debris during postnatal development may blunt the capacity of the cells to clear related debris later in life, possibly through long lasting receptor down regulation or selective cell elimination. Such changes in microglia would result in an environment that was less conducive to repair. Indeed, the higher levels of myelin debris, axon damage, and inflammation in LPC and EAE CID-treated animals strongly suggest environmental changes that compromise repair.

One surprising observation from the current study was that although there was an increase in the levels of activated microglia and reactive astrocytes in EAE animals that had been subjected to oligodendrocyte loss during development, this did not appear to significantly alter the course of the disease. For instance, neither the timing of onset nor the peak level of disease were significantly altered in animals subjected to neonatal CID exposure, which is in contrast to the differences in histology in the spinal cord of control

and CID treated animals. It is possible that the functional deficits seen in the MOG_{35-55} model are not directly a result of lesions in the spinal cord although this seems highly unlikely given the predominance of lesions are in the spinal cord [27, 28]. It is possible that the majority of the functional deficits result from insults to specific axon tracks in the spinal cord and that additional insult to adjacent cord regions has little additive effect even though it is clearly evident histologically. Indeed unlike LPC lesions that have distinct borders, EAE produces diffuse lesions [29] that are more challenging to quantify. It is also possible that the level of pathology induced by the MOG_{35-55} and pertussis toxin is sufficiently strong that the addition of a more subtle insult has no detectable impact on functionality. Decreasing the severity of EAE through use of a different model or reduction in the level of pertussis toxin stimulation may allow for the detection of incremental insults. Finally, in the EAE model the lack of repair may take an extended period of time to influence overall behavioral output and maintaining the animals for longer than 28 days post induction may have begun to reveal additional pathology. Further studies are required to clearly define the role of spinal cord inflammation in disease progression.

Conclusion

In conclusion, our data indicate that induction of apoptosis of mature oligodendrocytes early in development induces short and long term changes in the CNS microenvironment. The short term changers resolve within a few days but the long term changes persist in a primed state for many weeks/months and become evident following perturbation to the adult CNS. The concept of early priming provides a possible explanation and may explain how some individuals are more susceptible to develop certain diseases such as MS. Future studies will focus on defining the major cellular and molecular mechanisms mediating environmental changes following developmental oligodendrocyte ablation.

List Of Abbreviations

CID: chemical inducer of dimerization

CNS: central nervous system

EAE: experimental autoimmune encephalomyelitis

EOD: every other day

GA: glutaraldehyde

iCP9: inducible caspase 9

LPC: lysophosphatidylcholine

MBP: myelin basic protein

MOG: myelin oligodendrocyte glycoprotein

MS: multiple sclerosis

PBS: phosphate buffer saline

PFA: paraformaldehyde

PI: post-lesion

PS: phosphatidylserine

SEM: scanning electron microscopy

TG: transgenic

VEH: vehicle

Declarations

Acknowledgments

This work was supported by NS30800 and the Vivian Gill endowment from The George Washington University.

Ethical Approval and Consent to participate: Not applicable

Consent for publication: Yes

Availability of supporting data: Not applicable

Competing interests: Not applicable

Funding: 2R01NS030800

Authors' contributions: APG, designed and performed experiments, analyzed data and co-wrote the paper. **MK,** performed LPC surgeries. **EG,** processed tissues for SEM and prepared thick sections. **CCP,** performed SEM imaging. **JA,** helped with EAE behavioral scoring. **RHM,** designed experiments, analyzed data and co-wrote the paper.

Acknowledgements: This work was supported by NS30800 and the Vivian Gill endowment from The George Washington University

References

1. Kamel, F.O., *Factors Involved in Relapse of Multiple Sclerosis.* J Microsc Ultrastruct, 2019. **7**(3): p. 103-108.

2. Gluckman, P.D., et al., *Effect of in utero and early-life conditions on adult health and disease.* N Engl J Med, 2008. **359**(1): p. 61-73.
3. Sonnenberg, A. and V. Ajdacic-Gross, *Similar birth-cohort patterns in Crohn's disease and multiple sclerosis.* Mult Scler, 2018. **24**(2): p. 140-149.
4. Eagleton, M.J., et al., *Southern Association for Vascular Surgery William J. von Leibig Award. Inflammation and intimal hyperplasia associated with experimental pulmonary embolism.* J Vasc Surg, 2002. **36**(3): p. 581-8.
5. Dietert, R.R., J.M. Dietert, and J.C. Dewitt, *Environmental risk factors for autism.* Emerg Health Threats J, 2011. **4**: p. 7111.
6. Boisse, L., et al., *Long-term alterations in neuroimmune responses after neonatal exposure to lipopolysaccharide.* J Neurosci, 2004. **24**(21): p. 4928-34.
7. Bilbo, S.D., et al., *Neonatal infection induces memory impairments following an immune challenge in adulthood.* Behav Neurosci, 2005. **119**(1): p. 293-301.
8. Cunningham, C., et al., *Systemic inflammation induces acute behavioral and cognitive changes and accelerates neurodegenerative disease.* Biol Psychiatry, 2009. **65**(4): p. 304-12.
9. Hanamsagar, R. and S.D. Bilbo, *Environment matters: microglia function and dysfunction in a changing world.* Curr Opin Neurobiol, 2017. **47**: p. 146-155.
10. Caprariello, A.V., et al., *Apoptosis of oligodendrocytes in the central nervous system results in rapid focal demyelination.* Ann Neurol, 2012. **72**(3): p. 395-405.
11. Caprariello, A.V., et al., *Apoptosis of Oligodendrocytes during Early Development Delays Myelination and Impairs Subsequent Responses to Demyelination.* J Neurosci, 2015. **35**(41): p. 14031-41.
12. Pajoohesh-Ganji, A. and R.H. Miller, *Oligodendrocyte ablation as a tool to study demyelinating diseases.* Neural Regen Res, 2016. **11**(6): p. 886-9.
13. Pajoohesh-Ganji, A. and R.H. Miller, *Targeted Oligodendrocyte Apoptosis in Optic Nerve Leads to Persistent Demyelination.* Neurochem Res, 2019.
14. Polter, A., et al., *Deficiency in the inhibitory serine-phosphorylation of glycogen synthase kinase-3 increases sensitivity to mood disturbances.* Neuropsychopharmacology, 2010. **35**(8): p. 1761-74.
15. Quarles, R.H., *Myelin-associated glycoprotein (MAG): past, present and beyond.* J Neurochem, 2007. **100**(6): p. 1431-48.
16. Nakatsuji, Y. and R.H. Miller, *Density dependent modulation of cell cycle protein expression in astrocytes.* J Neurosci Res, 2001. **66**(3): p. 487-96.
17. Nakatsuji, Y. and R.H. Miller, *Control of oligodendrocyte precursor proliferation mediated by density-dependent cell cycle protein expression.* Dev Neurosci, 2001. **23**(4-5): p. 356-63.
18. Kotter, M.R., et al., *Myelin impairs CNS remyelination by inhibiting oligodendrocyte precursor cell differentiation.* J Neurosci, 2006. **26**(1): p. 328-32.
19. Robinson, S. and R.H. Miller, *Contact with central nervous system myelin inhibits oligodendrocyte progenitor maturation.* Dev Biol, 1999. **216**(1): p. 359-68.

20. Ravichandran, K.S., *Find-me and eat-me signals in apoptotic cell clearance: progress and conundrums.* J Exp Med, 2010. **207**(9): p. 1807-17.
21. Tyurin, V.A., et al., *Oxidatively modified phosphatidylserines on the surface of apoptotic cells are essential phagocytic 'eat-me' signals: cleavage and inhibition of phagocytosis by Lp-PLA2.* Cell Death Differ, 2014. **21**(5): p. 825-35.
22. Mueller, R.B., et al., *Attraction of phagocytes by apoptotic cells is mediated by lysophosphatidylcholine.* Autoimmunity, 2007. **40**(4): p. 342-4.
23. Novotna, K., et al., *Why patients with multiple sclerosis perceive improvement of gait during treatment with natalizumab?* J Neural Transm (Vienna), 2019.
24. Witcher, K.G., D.S. Eiferman, and J.P. Godbout, *Priming the inflammatory pump of the CNS after traumatic brain injury.* Trends Neurosci, 2015. **38**(10): p. 609-620.
25. Fenn, A.M., et al., *Immune activation promotes depression 1 month after diffuse brain injury: a role for primed microglia.* Biol Psychiatry, 2014. **76**(7): p. 575-84.
26. Ogura, H., et al., *Priming, second-hit priming, and apoptosis in leukocytes from trauma patients.* J Trauma, 1999. **46**(5): p. 774-81; discussion 781-3.
27. Pierson, E., et al., *Mechanisms regulating regional localization of inflammation during CNS autoimmunity.* Immunol Rev, 2012. **248**(1): p. 205-15.
28. Lefeuvre, J.A., et al., *The spectrum of spinal cord lesions in a primate model of multiple sclerosis.* Mult Scler, 2019: p. 1352458518822408.
29. McCarthy, D.P., M.H. Richards, and S.D. Miller, *Mouse models of multiple sclerosis: experimental autoimmune encephalomyelitis and Theiler's virus-induced demyelinating disease.* Methods Mol Biol, 2012. **900**: p. 381-401.

Table

Table 1. Mouse EAE Scoring (Based on Hooke Laboratories protocol)

Score	Clinical observations
0	Not different than non-immunized mouse. Tail has tension and is erect. Hind legs spread apart.
0.5	Tip of tail limp. The tail has tension except for the tip. Muscle straining is felt on the tail, while tail continues to move.
1	Limp tail. When picked up, tail drapes over finger. Hind legs spread apart. No signs of tail movement.
1.5	Limp tail and hind leg inhibition (one leg falls through wire rack). Walking is slightly wobbly.
2	Limp tail and weakness of hind legs. Legs not spread apart. Apparent wobbly walk. Toe dragging in one foot. *OR* head tilting. Poor balance
2.5	Limp tail and dragging of hind legs. Both hind legs have movement but mouse trips on hind feet. *OR* no movement in one leg/completely drags one leg, but movement in other leg. *OR* EAE severity is mild but a strong head tilt that causes the mouse to occasionally fall over.
3	Limp tail and complete paralysis of hind legs. *OR* one or both hind legs are able to paddle but not able to move forward. *OR* almost complete paralysis of hind legs. Limp tail and paralysis of one front and one hind leg. *OR* severe head tilting, walking at the end of the cage, pushing against the cage wall, spinning when pick up at the base of the tail.
3.5	Limp tail and complete paralysis of hind legs. Mouse moving but when place on its side unable to right itself. Hind legs are together on one side of the body. *OR* Mouse moving but the hind quarters are flat like a pancake, giving the appearance of a hump in the front quarters of the mouse.
4	Limp tail. Complete hind leg and partial front leg paralysis. Mouse not moving much but appears alert and feeding. Euthanasia is recommended. Euthanize if mouse scores 4 for 2 days. With daily SC fluid most C57B may recover to 3.5 or 3.
4.5	Complete hind leg and partial front leg paralysis. No movement. Mouse is not alert and barley responds to contact. Euthanasia is recommended.
5	Mouse is spontaneously rolling in the cage. Mouse is dead or euthanized due to severe paralysis.

Figures

Figure 1

Systemic CID injection induces loss of DsRed+ oligodendrocytes and a decrease in MBP staining throughout the CNS. Sections of tissues taken one day after the final injection of CID (P4-P11) show reduction in the number of oligodendrocytes and myelin throughout the CNS. Corpus callosum (A), cerebellum (B), optic nerve (C), and spinal cord (D) sections from MBP-iCP9 transgenic mice subcutaneously injected with vehicle (VEH) or CID were labeled with antibodies to MBP (green), DsRed (red), and DAPI (blue). The bottom panel in each image shows the areas indicated with the white asterisk in the top panel (Bar = 25 μm).

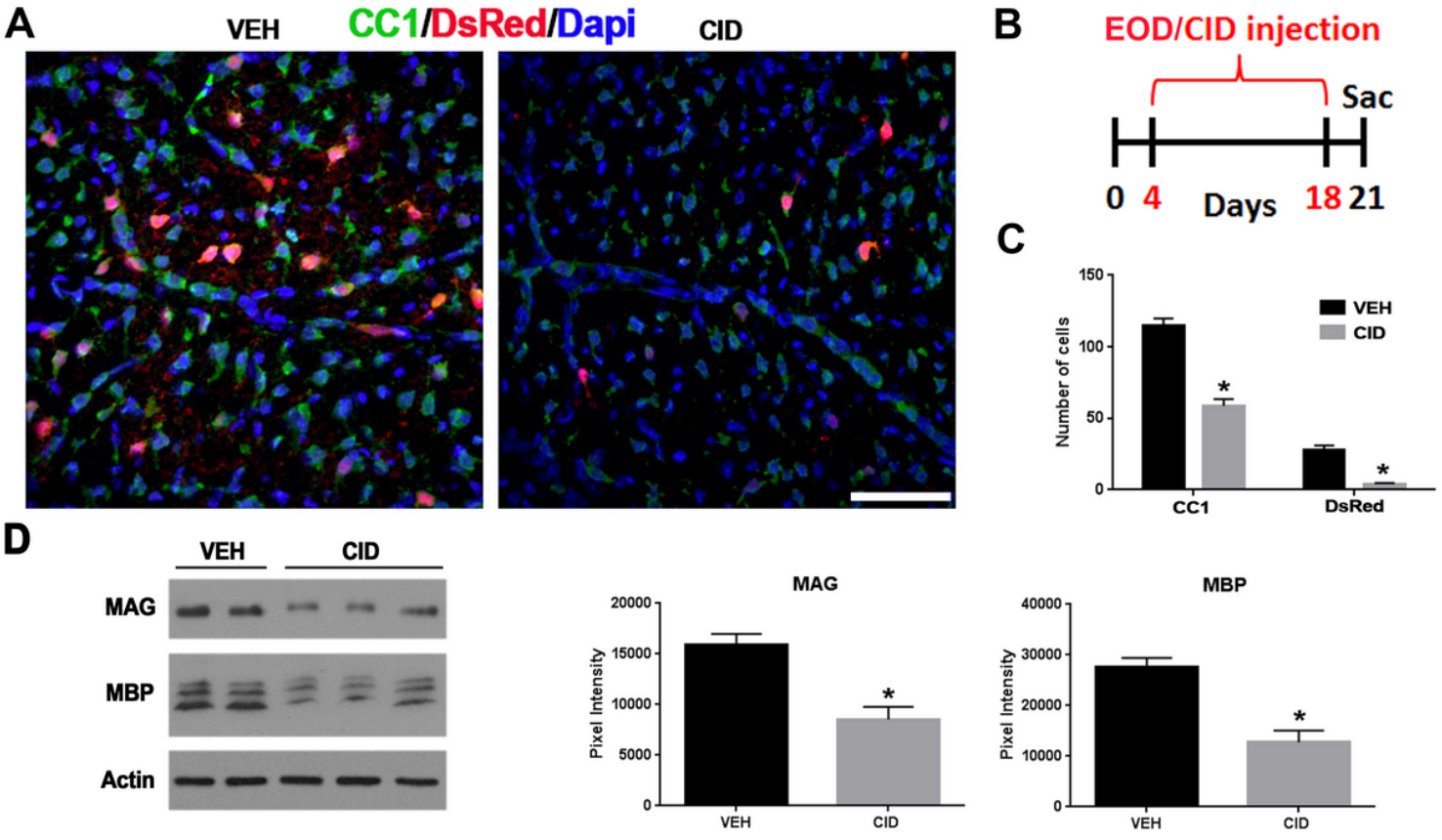

Figure 2

Oligodendrocyte ablation results in a significant decrease in mature oligodendrocytes and a decrease in myelin proteins. A. Representative images of spinal cord sections labeled with antibodies to CC1 (green), DsRed (red), and DAPI (blue) in vehicle (VEH) and CID injected pups. Note that the CID injected animals show a significant decrease in CC1 and DsRed staining. B. Schematic of the CID injection and tissue collection. C. Quantification of cell numbers indicate a significant decrease (p-value = 0.001) in the number of mature CC1+ oligodendrocytes and DsRed+ cells in CID-injected animals. D. Western blot analysis of spinal cord tissue indicates that the myelin proteins MAG (p-value = 0.007) and MBP (p-value = 0.005) were decreased significantly after CID injection (Bar = 25 μm).

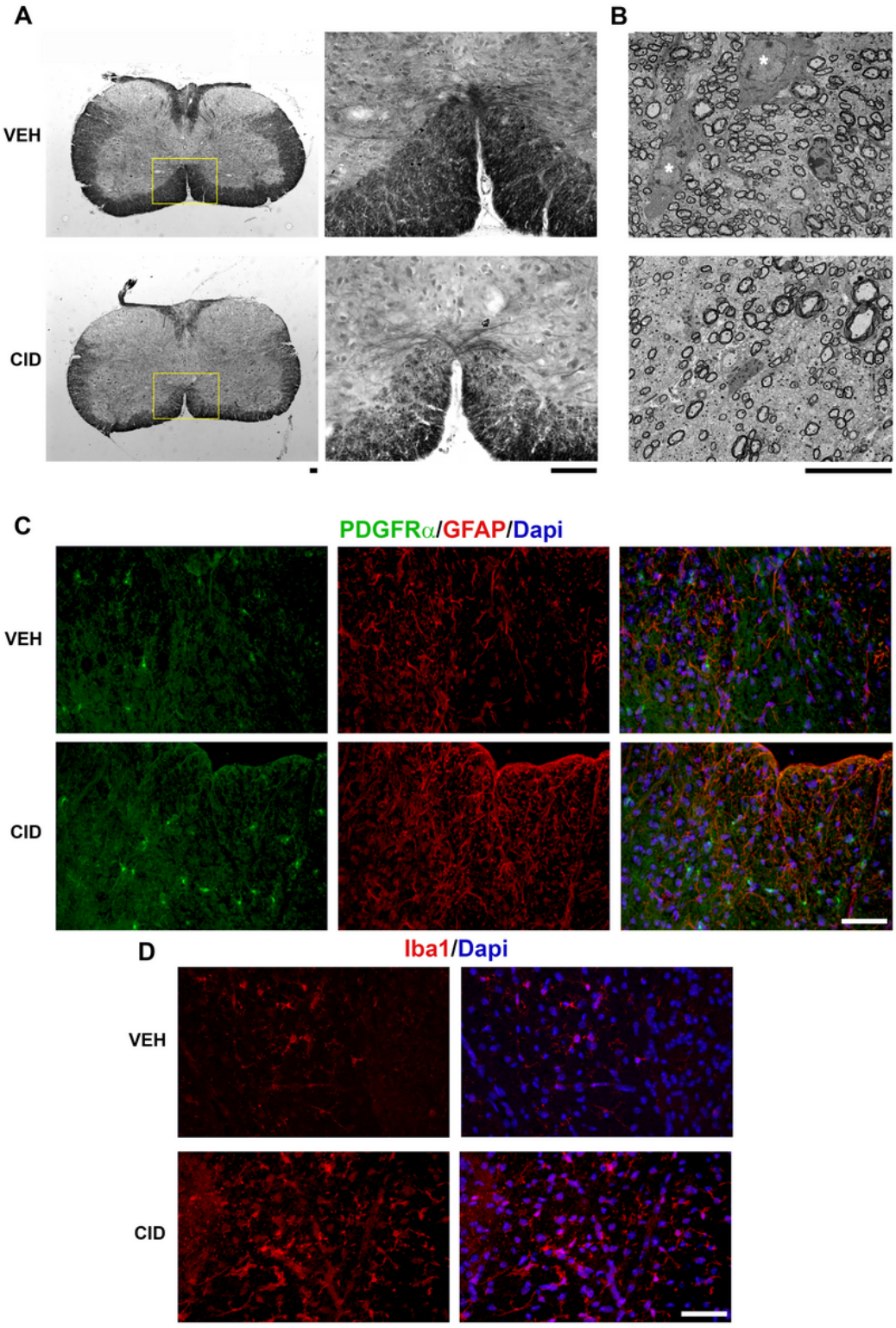

Figure 3

Early oligodendrocyte ablation results in a decrease in myelinated axons, an increase in astrocytes and microglial activation, and elevated numbers of oligodendrocyte progenitor cells. A. Representative images of spinal cord sections stained with Solochrome indicate a decrease in myelin staining observed throughout the white matter in animals exposed to CID compared to vehicle treated controls. The areas in yellow boxes have been magnified. B. EM sections confirmed the decrease in myelinated axons in CID

compared to vehicle treated spinal cord. Healthy oligodendrocytes (white asterisk) are apparent in the vehicle (VEH) treated image associated with neighboring axons. C. Oligodendrocyte ablation results in changes in adjacent neural cell populations. Sections from spinal cord injected with VEH or CID were labeled with antibodies to PDGFRα (green), GFAP (red), Iba1 (red in D), and Dapi (blue). Glial activation and OPCs proliferation is seen after CID injection (Bar = 10 μm in A and B, Bar = 25 μm in C).

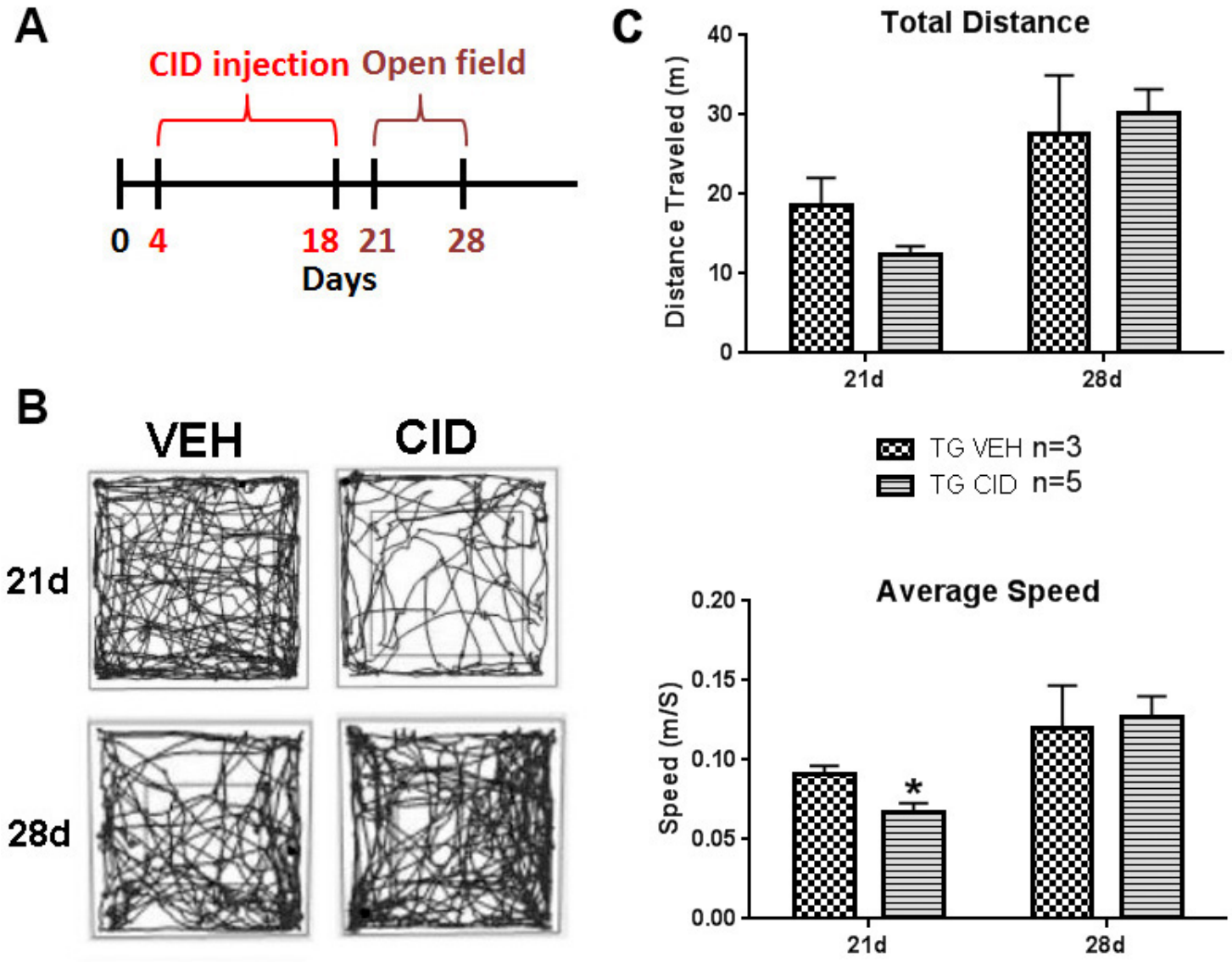

Figure 4

Oligodendrocytes ablation results in a transient functional deficit. A. Schematic of the CID injection and open filed testing. B. Representative traces obtained from mice 21 (3 days post-CID) and 28 (10 days post-CID) days after birth. At 21 days (3dpl) the motility of the animals is significantly lower following CID injection than in vehicle treated controls as indicated by the number of traces. One week later the level of motility between the two groups was similar. C. Quantification of the differences in total distance and average speed traveled indicates a decrease in total distance and a significant decrease (p-value = 0.03) in average speed traveled in CID-treated mice at 21 days, which is absent at 28 days.

Figure 5

Relative lesion area of LPC induced demyelination is larger in CID-treated mice than controls. A. Schematic of the CID injection and the time line for LPC injections. B. Representative images show sections from wild type mouse injected with saline (WT/-/Saline), MBP-iCP9 transgenic mouse injected with vehicle followed by LPC (TG/VEH/LPC), and MBP-iCP9 transgenic mouse injected with CID followed by LPC (TG/VEH/LPC). Sections were taken 14 days after LPC injection. WT mice injected with saline did not show any signs of lesion. WT/CID/LPC and TG/VEH/LPC treated mice (Control) both served as control groups in which oligodendrocytes were not ablated. C. The total volume of white matter (WM) area was compared to the total volume of spinal cord across all groups and no significant differences were detected suggesting that normal myelination was unaffected by creation of the transgenic phenotype. The relative proportion of dorsal white matter with lesion was significantly (p-value = 0.004) higher in experimental transgenic mice, that had received CID and LPC compared to those that received vehicle and LPC or wild type mice that received CID, which may reflect slower remyelination in the CID-treated transgenic mice (Bar in B =25 μm).

Figure 6

Remyelination is reduced in LPC induced demyelination in CID-treated transgenic mice. Vehicle and CID treated MBP-iCP9 transgenic mice were injected with LPC at 6 weeks of age (about 4 weeks after the last CID injection). Sections were stained using Toluidine Blue stain (upper panels) and remyelinated axons were counted in three regions in the dorsal column. There is a significant decrease (p-value = 0.02) in the number of remyelinated axons indicating decreased recovery in the CID treated mice. Lower panels show the SEM images. Note the lower level of myelinated axons and the presence of foamy macrophages in the CID-treated tissue as indicated by the white ¬asterisk (Bar = 10 μm).

Figure 7

CID-treated animals have worse histological outcomes in EAE which is not However, the tissue integrity (D) was worse in the CID-treated with a greater degree of myelin perturbation and axonal degeneration ¬¬¬¬(Bar = 5 μm).

Figure 8

Astrocyte activation is increased in the CNS of animals with EAE that were subjected to developmentally oligodendrocyte ablation. Sections from spinal cord of EAE mice treated developmentally with vehicle or CID were labeled with GFAP (green) and Dapi (blue). Bottom panels show higher magnifications (63x) of the areas indicated by asterisks in the lower magnification (25x) images in the top panels. The higher magnification areas are taken from (top to bottom) the dorsal (D), near the central canal (C), and ventral

(V) spinal cord. Astrocytes are more activated in the CID-treated tissues as indicated by the increase in the number and the thickness of astrocytic processes stained with GFAP (Bar =25 μm).

Figure 9

Microglial activation is increased in the CNS of animals with EAE subjected to developmentally oligodendrocyte ablation. Sections from spinal cord of EAE mice treated developmentally with vehicle or CID were labeled with antibody to Iba1 (a microglial marker, red) and Dapi (blue). Bottom panels show higher magnifications (63x) of the areas indicated by asterisks in the lower magnification (25x) images in the bottom panels. The higher magnification areas are taken from (top to bottom) dorsal (D), near the central canal (C), and ventral (V) spinal cord. The increase in the number and morphology of the microglia is evident in the CID-treated tissues as indicated by the change in the staining intensity and the morphology of the microglia from more ramified in the VEH-treated to more amoeboid in the CID-treated tissues (Bar = 25 μm).